Supplemental material for

# BCL6 confers *KRAS*-mutant non-small-cell lung cancer resistance to BET inhibitors

Jiawei Guo[1,2,6], Yanan Liu[1,6], Jing Lv[1,6], Bin Zou[3], Zhi Chen[1,4], Kun Li[1], Juanjuan Feng[1], Zhenyu Cai[5], Lai Wei[3], Mingyao Liu[1], Xiufeng Pang[1,*]

[1] Shanghai Key Laboratory of Regulatory Biology, Institute of Biomedical Sciences and School of Life Sciences, East China Normal University, Shanghai 200241, China; [2] Department of Thoracic Surgery, State Key Laboratory of Biotherapy and Cancer Center, West China Hospital, Sichuan University and Collaborative Innovation Center for Biotherapy, 610041, Chengdu, China; [3] State Key Laboratory of Ophthalmology, Zhongshan Ophthalmic Center, Sun Yat-sen University, Guangzhou 510060, China; [4] Medical Research Institute, Wuhan University, Wuhan 430071, China; [5] Tongji University Cancer Center, Shanghai Tenth People's Hospital, School of Medicine, Tongji University, Shanghai 200092, China.

[6] These authors contributed equally to this work.

To whom correspondence should be addressed:
Dr. Xiufeng Pang
Institute of Biomedical Sciences and School of Life Sciences
East China Normal University
500 Dongchuan Rd.
Shanghai 200241, China
Office phone: +86-21-24206942
Office fax: +86-21-54344922
E-mail: xfpang@bio.ecnu.edu.cn

The authors have declared that no conflict of interest exists.

# This supplementary material contains

**Supplementary Figure 1**

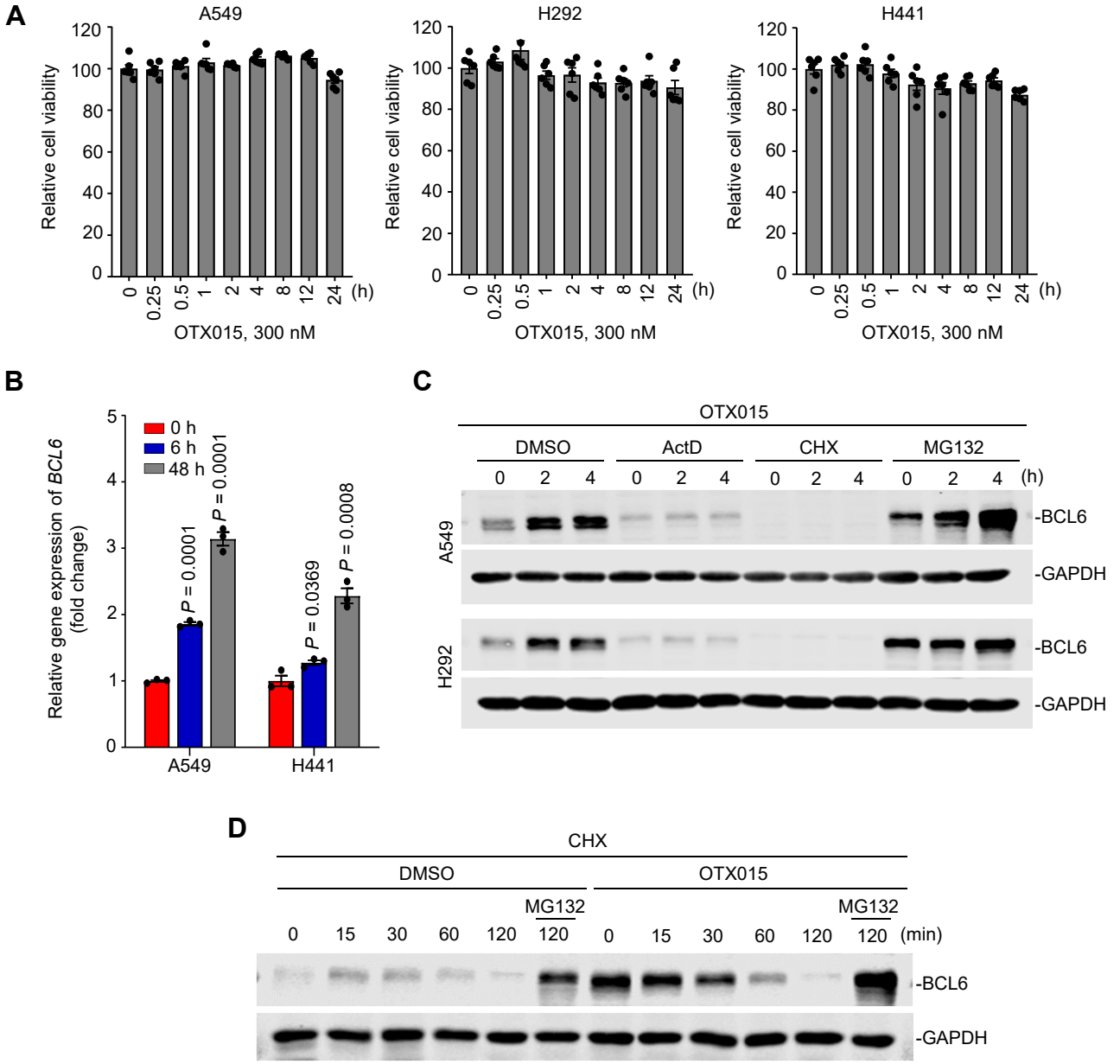


**Supplementary Figure 1 | OTX015 enhances BCL6 transcription. (A)** OTX015 (300 nM) did not induce cell death at indicated time points. Bar graphs represent the mean ± s.e.m. of six biological replicates. **(B)** OTX015 upregulated BCL6 mRNA level. A549 and H441 cells were treated with 300 nM OTX015 for indicated times. BCL6 mRNA levels were measured by qPCR assays. Data is expressed as mean ± s.e.m. of biological triplicates. *P* values were analyzed by comparing OTX015 treatment groups with the untreated group using unpaired, two-tailed Student's *t*-test. **(C)** OTX015-mediated upregulation of BCL6 was due to increased BCL6 transcription. A549 and H292 cells were respectively pre-treated with DMSO (1%), actinomycin D (ActD, 5 μM), cycloheximide (CHX, 25 μg/mL) or MG132 (10 μM) for one hour, followed by treatment with 300 nM OTX015 for indicated time intervals. Cells were collected and subjected to Western blotting analysis. **(D)** OTX015 did not affect protein degradation rate of BCL6. H292 cells were treated with or without 300 nM OTX015 for 24 h, followed by treatment with 25 μg/mL CHX for indicated periods, with or without MG132 (10 μM) treatment. Cells were collected and probed with antibodies against BCL6 and loading control GAPDH. The blots are representative of at least three independent experiments.

**Supplementary Figure 2**

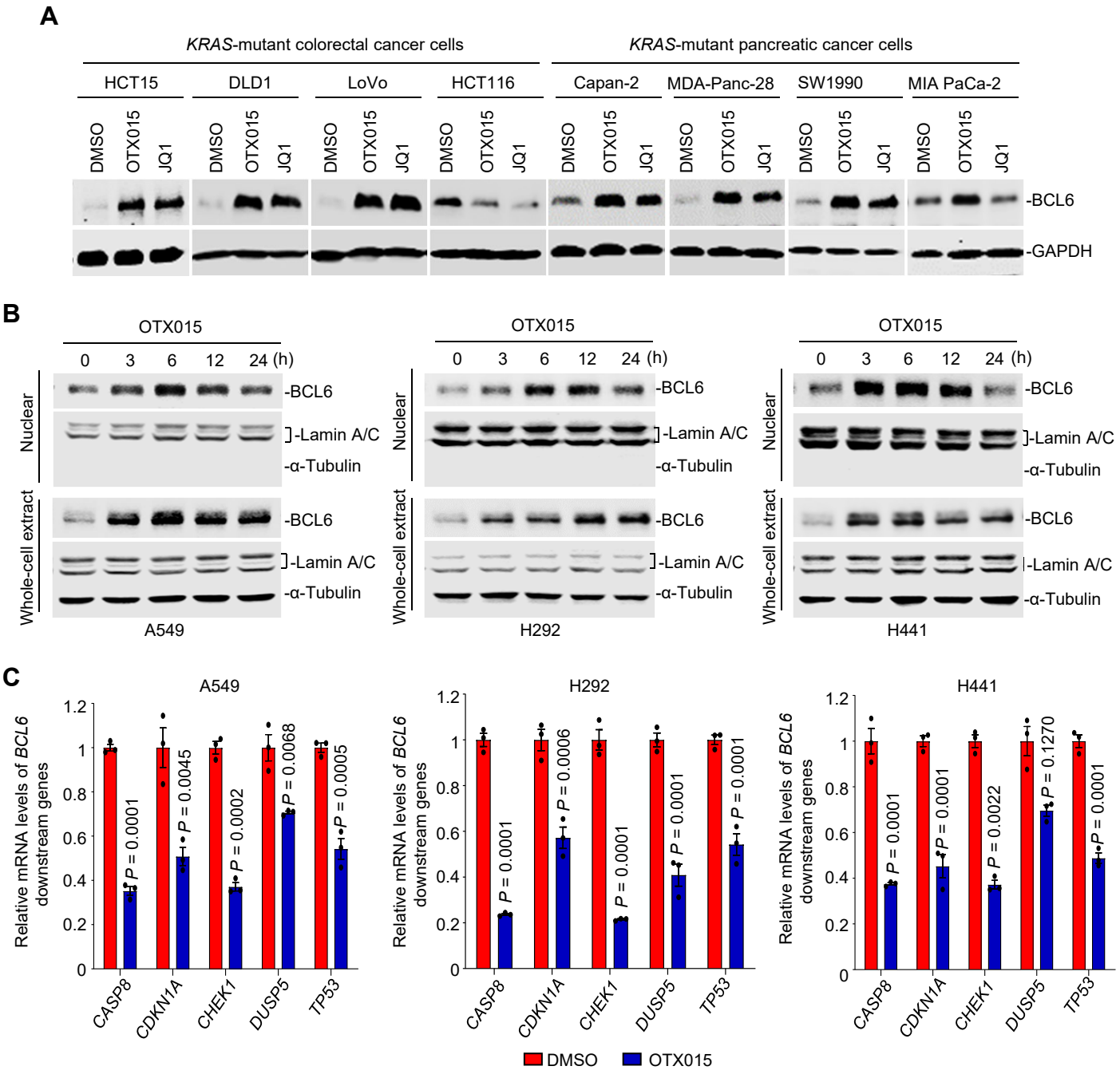


**Supplementary Figure 2 | BET inhibitors activate BCL6 and its target genes. (A)** BET inhibitors upregulated BCL6 expression across *KRAS*-mutant colorectal and pancreatic cancer cell lines. Cells were treated with OTX015 (300 nM) or JQ1 (300 nM) for 6 h. Treated cells were then harvested for immunoblotting analysis. **(B)** BCL6 expression in nuclear and whole cell extract in response to OTX015 treatment. A549, H292 and H441 cells were treated with 300 nM OTX015 for indicated periods. Treated cells were subsequently fractionated into nuclear and whole cell extract, followed by immunoblotting with antibodies against BCL6, α-tubulin and Lamin A/C (loading control). The blots are representative of at least three independent experiments. For each cell line, BCL6 in nuclei and BCL6 in whole-cell extract are contemporaneous immunoblots from the same biological replicate. **(C)** Expression of putative BCL6 downstream target genes mediated by OTX015 treatment. A549, H292 and H441 cells were exposed to 300 nM OTX015 for 48 h. Target gene transcription from each treatment was determined by qPCR. Relative gene expression was normalized to GAPDH level. Data is expressed as mean ± s.e.m. of biological triplicates. *P* values were analyzed by comparing OTX015 treatment group with the untreated group using unpaired, two-tailed Student's *t*-test.

**Supplementary Figure 3**

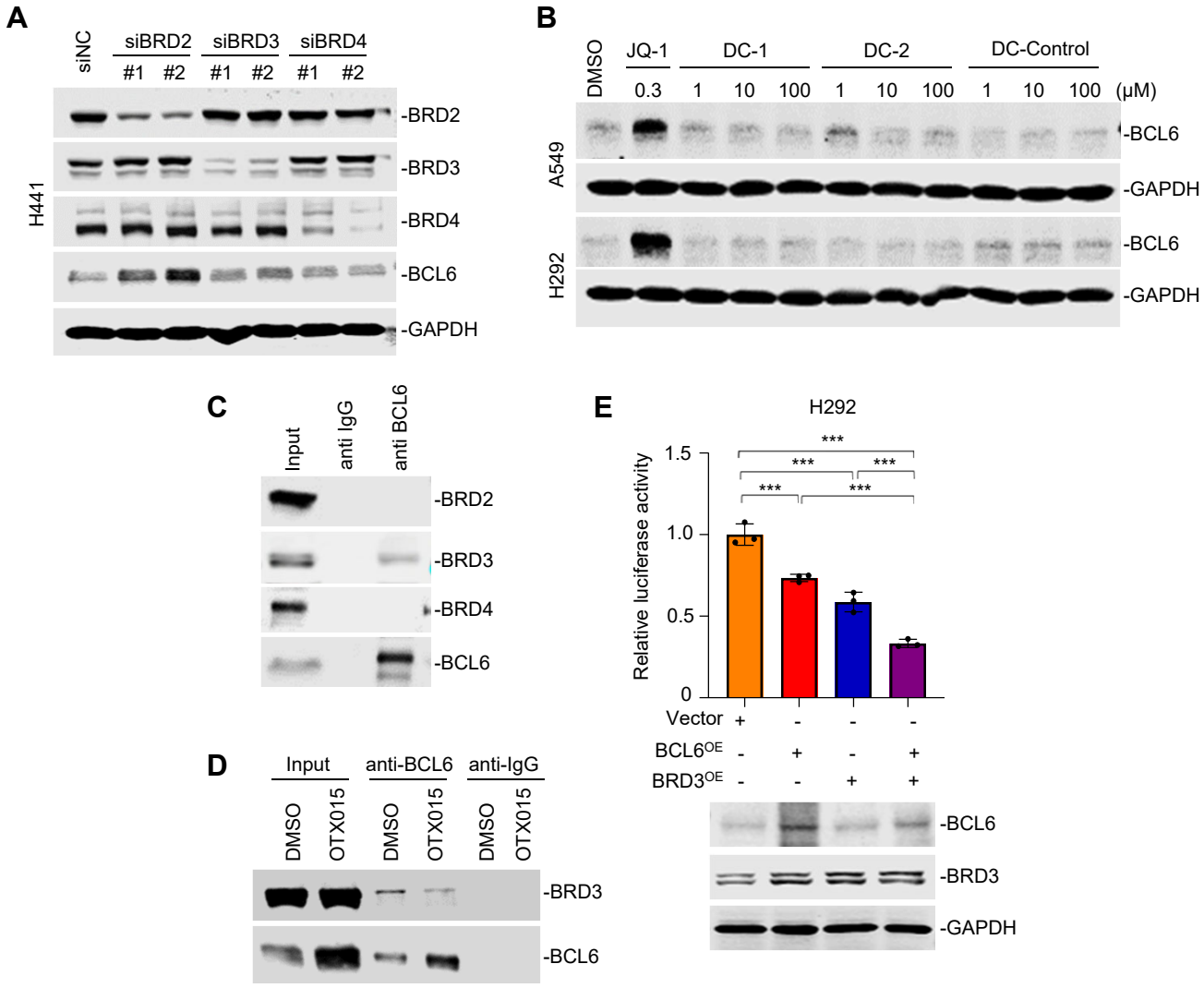


**Supplementary Figure 3 | OTX015 enhances BCL6 transcription in a BRD3-dependent manner. (A)** The impacts of BRD2, 3, 4 knockdown on BCL6 expression. H441 cells were transfected with indicated siRNAs targeting BRD2, BRD3 and BRD4 for 48 h, respectively. Cells were then harvested for Western blotting analysis. The knock-down efficiency was determined by BRD2/3/4 antibodies in parallel. **(B)** Specific BRD4 inhibitors showed limited effects on BCL6 expression. A549 and H292 cells were treated with indicated concentrations of JQ1 or DC compounds for 6 h. Cells were collected and probed with antibodies against BCL6. **(C)** Endogenous interaction of BCL6 and BRD3. H441 cell lysates were subjected to immunoprecipitation using an anti-BCL6 antibody. Immunoprecipitates were analyzed with antibodies against BRD2, BRD3, BRD4 and BCL6. Ten percent of total lysate was used as input control. Anti-IgG antibody was used as a negative control. **(D)** Endogenous interaction of BCL6 and BRD3 were decreased by OTX015 treatment. A549 cell lysates were subjected to immunoprecipitation using an anti-BCL6 antibody. Immunoprecipitates were analyzed with antibodies against BRD3. Ten percent of total lysate was used as input control. Anti-IgG antibody was used as a negative control. **(E)** BRD3 participated in BCL6 autoregulation circuit. H292 cells were co-transfected with P1-Fluc, together with equivalent amount of pcDNA3.1-BRD3, pcDNA3.1-BCL6 and/or pcDNA3.1-Ctrl as indicated. Cells were harvested for luciferase assay 48 h post-transfection. Western blotting was conducted by using antibodies against BCL6 and BRD3. Data is expressed as mean ± s.d of biological triplicates. *P* value was analyzed by one-way ANOVA as indicated. *** $P < 0.001$**.** Immunoblots in **A**, **C**, **D** and **E** were contemporaneous and ran in parallel from the same biological replicate. All immunoblots are representative of at least three independent experiments.

**Supplementary Figure 4**

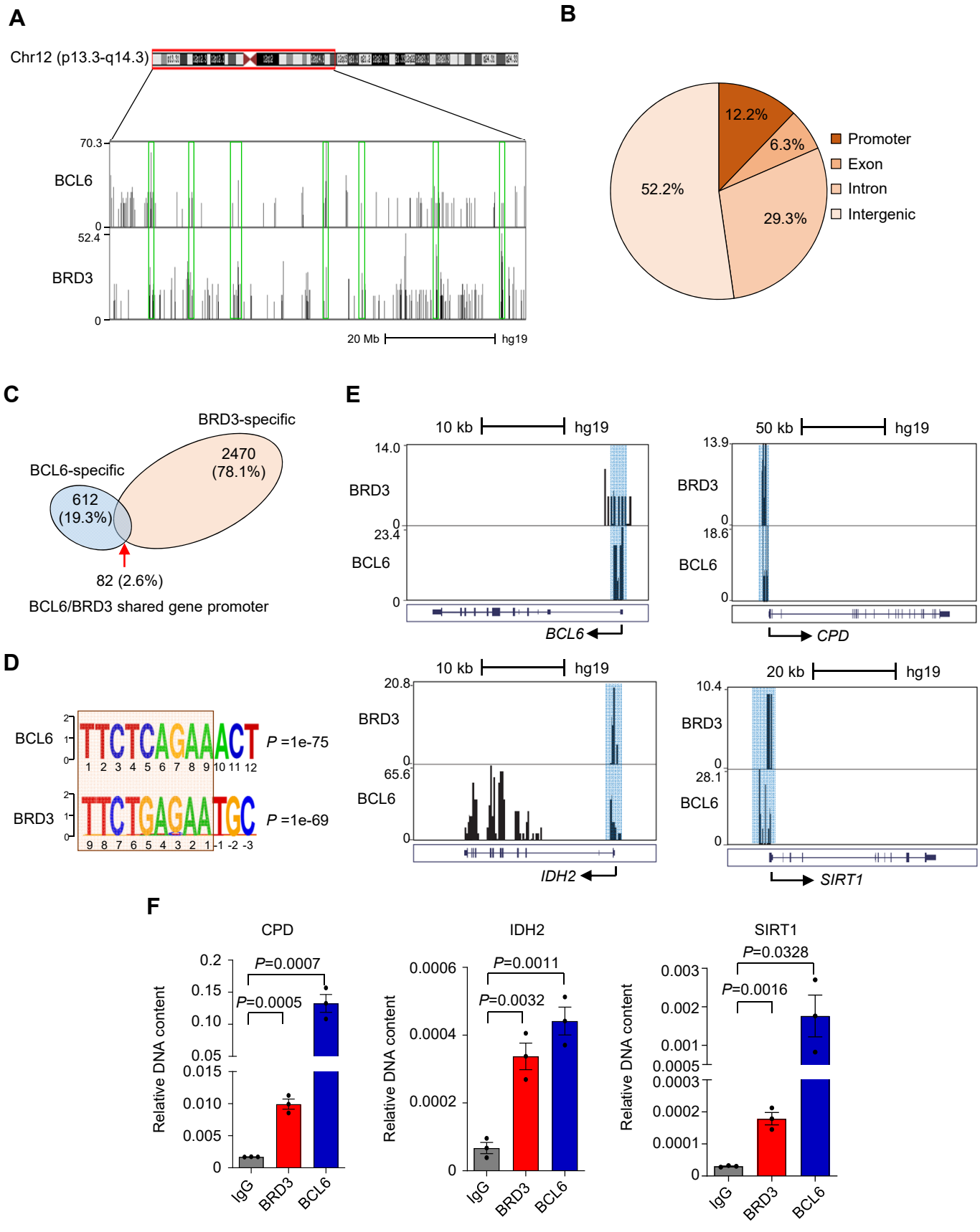

**Supplementary Figure 4 | BRD3 and BCL6 show similar binding preference. (A)** ChIP-seq binding tracks for BRD3 and BCL6 at selected chromosome 12 regions in untreated A549 cells. Green frames represent the co-localization of peaks. **(B)** Distribution of BCL6/BRD3 co-occupancy in proximal promoter, exon, intron, and intergenic regions. **(C)** Venn diagram showing the overlap of BCL6- and BRD3-binding gene promoters in untreated A549 cells. Red arrow marks the amount and percentage of gene promoters with both BCL6 and BRD3 binding. **(D)** Comparison of BCL6-binding motifs with BRD3-binding motifs in A549 cells. The consensus binding sequences at the promoter were identified by HOMER. *P* values represent enrichment of BCL6 or BRD3 compared to background. (**E**) BCL6- and BRD3-colocalized peaks located at several gene loci including *BCL6*, *CPD*, *IDH2* and *SIRT1* were shown. Blue shading marks the peaks located in the promoter region. **(F)** BCL6 and BRD3-colocalized peaks in the promoter regions of *CPD*, *IDH2* and *SIRT1* genes were examined by ChIP-qPCR. Data is expressed as mean $\pm$ s.e.m. of biological triplicates. *P* values were analyzed by comparing gene enrichment in BRD3 or BCL6 with IgG precipitations using unpaired, two-tailed Student's *t*-test.

**Supplementary Figure 5**

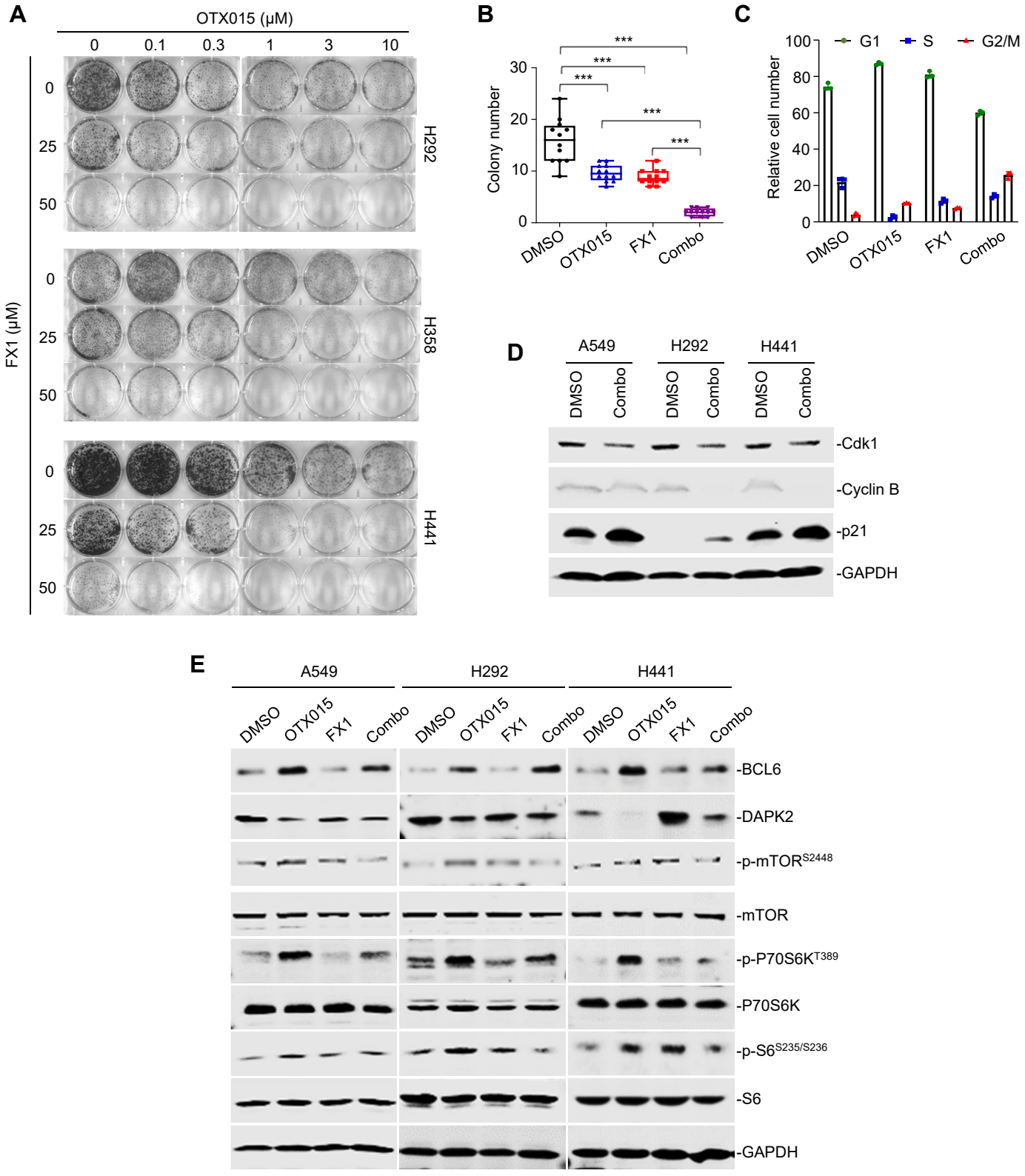

**Supplementary Figure 5 | BCL6 inhibitor sensitizes *KRAS*-mutant NSCLC cells to BET inhibitors in vitro. (A)** Clonogenic images of *KRAS*-mutant NSCLC cells treated with OTX015, FX1 or both drugs. Images are representative of three independent experiments. **(B)** Quantification of 3D-clonogenic formation assay of A549 cells, related to **Fig.6B**. Colony number (12 picked fields for each experimental group) was shown. The horizontal lines representing the median, and the bottom and top of the boxes represent the 25$^{th}$ and 75$^{th}$ percentiles, respectively. The vertical bars represent the range of the data. *** $P < 0.001$, by one-way ANOVA. **(C)** Cell cycle distribution of H441 cells upon indicated treatments. Data is expressed as mean ± s.d. of biological triplicates. **(D)** Cell cycle-related proteins affected by the combination treatment. A549, H292 and H441 cells were treated with or without the combined regime of OTX015 (300 nM) and FX1 (25 μM) for 48 h. Cells were collected and probed with antibodies against Cdk1, Cyclin B, p21 and loading control GAPDH. **(E)** Effects of OTX015 and FX1 combination treatment on the mTOR signaling pathway in *KRAS*-mutant lung cancer cells. A549, H292 and H441 cells were treated with 300 nM OTX015 alone or together with 15 μM FX1 for 48 h. Cells were collected and probed with antibodies against BCL6, DAPK2, p-mTOR$^{S2448}$, mTOR, p-P70S6K$^{T389}$, P70S6K, p-S6$^{S235/S236}$ and S6. GAPDH served as the loading control. The blots in **D** and **E** were contemporaneous from the same biological replicate, and are representative of at least three independent experiments.

**Supplementary Figure 6**

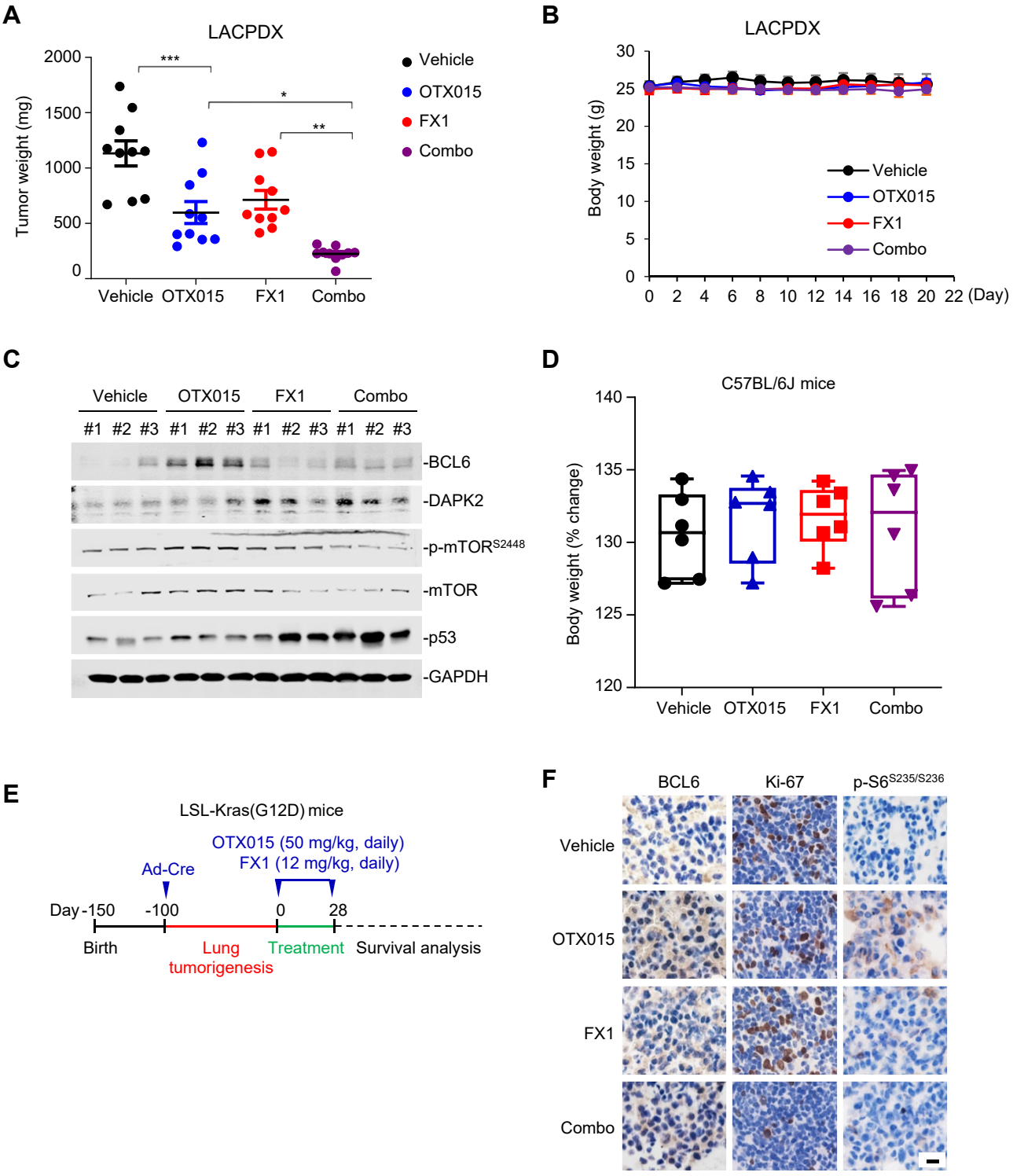

**Supplementary Figure 6 | In vivo efficacy of OTX015 and FX1 combination. (A)** Mean of tumor weight at day 21 (n=10 per group). Each dot represents a tumor from an individual mouse. Values are mean ± s.e.m.. * $P < 0.05$, ** $P < 0.01$, *** $P < 0.001$, by one-way ANOVA analysis. **(B)** Mouse body weight of the LACPDX mice. Values are mean ± s.e.m.. **(C)** Western blotting analysis of BCL6 and its downstream signaling components in LACPDX tumors. At the end of the treatment, PDX tumors were isolated from different mice and tumor lysates were immunoblotted. **(D)** Box plots showing the fold change of body weight of C57BL/6J normal mice at day 28 (n = 6), relative to mouse body weight on the first day of treatment. The horizontal lines representing the median, and the bottom and top of the boxes represent the $25^{th}$ and $75^{th}$ percentiles, respectively. The vertical bars represent the range of the data. **(E)** Treatment schedule for administration of FX1 and OTX015 in the LSL-Kras(G12D) mouse model. **(F)** Representative immunohistochemical images of BCL6, Ki-67 and p-$S6^{S235/S236}$ in tumors isolated from LSL-Kras(G12D) mice at day 28. Scale bars, 10 μm.

**Supplementary Figure 7**

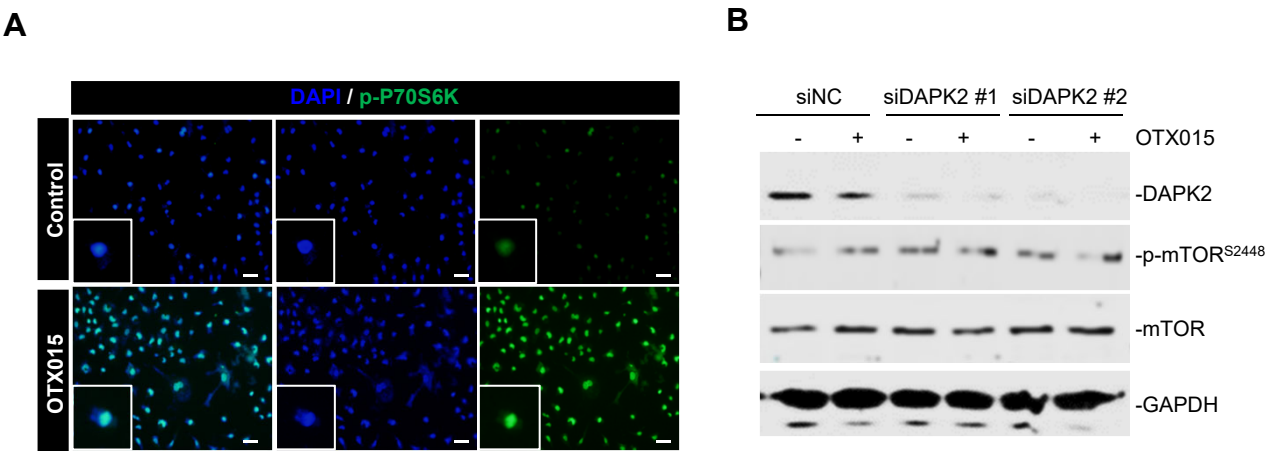


**Supplementary Figure 7 | OTX015-mediated mTOR signaling activation is dependent on DAPK2.** **(A)** Phospho-P70S6K$^{T389}$ level was broadly increased upon OTX015 treatment in cells. A549 cells were treated with 300 nM OTX015. Immunofluorescence of p-P70S6K$^{T389}$ was subsequently conducted. Scale bars, 50 μm. **(B)** Genetic silencing of DAPK2 expression prevented mTOR activation in the presence of OTX015. A549 cells were transfected with DAPK2 siRNA or empty vector control and then treated with 300 nM OTX015 for 48 h. Treated cells were tested by immunoblotting with indicated antibodies. The blots are representative of at least three independent experiments.

**Supplementary Figure 8**

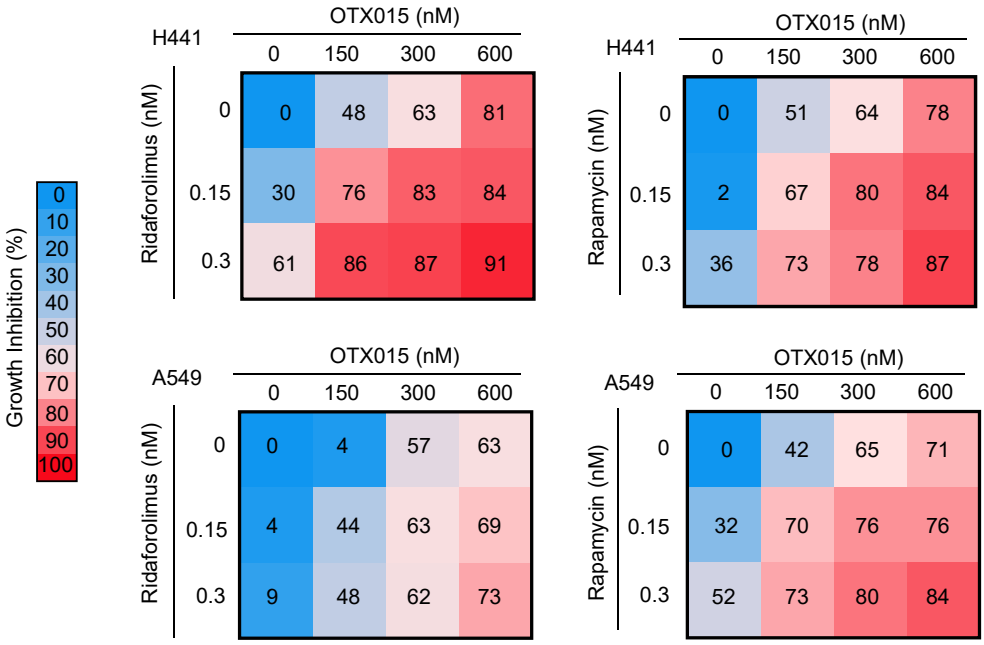


**Supplementary Figure 8 | A synergistic effect of BETi and mTORi on viability of cultured colonies.** A549 and H441 cells were respectively treated with indicated concentrations of OTX015, ridaforolimus, rapamycin or their combinations. Two-dimensional clonogenic assay was conducted, where culture medium with or without drugs was replaced every other day. Percentage of growth inhibition was quantified by setting vehicle-treated group as 0. Data are presented as average mean of three independent experiments.

## SUPPLEMENTAL METHODS

**Reagents.** Abemaciclib (S7158, CDK4/6 inhibitor), Bortezomib (S1013, 20S proteasome inhibitor) Dacomitinib (S2727, EGFR inhibitor), Defactinib (S7654, FAK inhibitor), Momelotinib (S2219, JAK1/JAK2 inhibitor), OTX015 (S7360, BET bromodomain inhibitor), Ridaforolimus (S1022, mTOR inhibitor), Selumetinib (S1008, MEK1 inhibitor), Tivantinib (S2753, c-MET inhibitor), Docetaxel (S1148, microtubule association inhibitor), I-BET762 (S7189, BET bromodomain inhibitor), AZD5153 (S8344, BET bromodomain inhibitor) and BI7273 (S8179, BRD9 bromodomain inhibitor) were purchased from Selleckchem. Retaspimycin (HY-15263, HSP90 inhibitor), cis-diamine dichloroplatinum (CDDP, HY-17394, DNA synthesis inhibitor) and Actinomycin D (HY-17559) were purchased from MedChemExpress. (+)-JQ1 (S7110, BET bromodomain inhibitor) was kindly provided by J. Bradner (Harvard Medical School) or purchased from Selleckchem. DC-1, DC-2 and DC-control were kindly provided by Dr. Cheng-Ming Chiang (University of Texas Southwestern Medical Center, Dallas, TX). BI3802, FX1 and Compound 7 were synthesized and kindly provided by Dr. Yihua Chen (East China Normal University, Shanghai, China).

**RNA interference.** BET protein knockdown and BCL6 knockdown were achieved by RNA interference using the following siRNAs: siBRD2 #1: CCCTGCCTACAGGTTATGATT, siBRD2 #2: CCTATGGACATGGGTACTATT; siBRD3 #1: GCTGATGTTCTCGAATTGCTA, siBRD3 #2: CCAAGGAAATGTCTCGGATAT; siBRD4 #1: CCTGGAGATGACATAGTCTTA, siBRD4 #2: GCCAAATGTCTACACAGTATA; siBCL6 #1: CCTTGTGACAAGGCCAGCA, siBCL6 #2: CCAUUGUGAGAAGUGUAACCUGCAU; siDAPK2 #1: GTTACGACTTTGATGAGGAAT; siDAPK2 #2:CACGAAATAGAAGATGGAGTT. Briefly, cells were transfected with 200 pmol siRNA for 48 h before harvesting. Cell lysates were subjected to Western blotting analysis.

**Western blotting analysis.** Western blotting was performed using standard methods. Briefly, whole-cell lysates or tumor tissue extracts were lysed in radio-immunoprecipitation assay buffer (150 mM sodiumchloride, 50 mM Tris pH 8.0, 1% Triton X-100, 0.5% sodium

deoxycholate, 0.1% sodium dodecyl sulfate (SDS)) supplemented with protease and phosphatase inhibitors (MedChemExpress). Lysates were centrifuged at 12,000 rpm. for 20 min at 4 °C, and the supernatants were collected. For the nuclear extracts, cells were collected in four volumes of lysis buffer (10 mM HEPES, pH 7.9, 10 mM KCl, 0.1 mM ethylenediaminetetraacetic acid, 0.1 mM ethylene glycol tetraacetic acid) and incubated on ice for 15 min. Then, 1/16$^{th}$ volume of 10% NP-40 (final concentration of 0.625%) was added to the cell lysates, which were subsequently vortexed for 10 s, and incubated on ice for 2 min. After centrifugation (16000 g, 15 min, 4 °C), the cell pellets were re-suspended in nuclear lysis buffer (150 mM NaCl, 0.1% Tween-20, 50 mM HEPES, pH 7.3), and incubated on ice for 20 min. After centrifugation (20000 g, 15 min, 4 °C), the supernatants were subjected to nuclear protein analysis. Protein concentration of supernatants was determined using BCA protein assay kit (Thermo Scientific). Equal amounts (50-80 μg) of the proteins were separated by 8–12% SDS–polyacrylamide gel electrophoresis gels and transferred to nitrocellulose membranes (Millipore). Membranes were blocked in Tris Buffered saline with Tween (TBS-T)/5% (w/v) bovine serum albumin for 1 h at room temperature, and then incubated with primary antibodies for Western blotting analysis at 4 °C overnight. The membranes were washed with PBS-T and incubated with anti–mouse IgG or anti–rabbit IgG (1:10000 dilution) for 1 h at room temperature. Signal on the membranes was detected using the Odyssey Infrared Imaging System (Odyssey, LI-COR). The following antibodies were used: Anti-BCL6 (#14895), anti-Lamin A/C (#2032), anti-BRD2 (#5848), anti-BRD4 (#13440), anti-phospho-mTOR$^{S2448}$ (#2971), anti-mTOR (#2972), anti-phospho-p70 S6K$^{T389}$ (#9206), anti-p70 S6K (#9202), anti-phospho-4E-BP1$^{T37/T46}$ (#2855), anti-4E-BP1 (#9644), anti-p21 (#2947), anti-p53 (#9282) and anti-phospho-S6$^{S235/S236}$ (#2211) antibodies were purchased from Cell Signaling Technology. Anti-alpha-Tubulin (#1878-1), anti-GAPDH (#ab181602), anti-Cdk1 (#3787-1) and anti-Ki67 (#ab16667) antibodies were purchased from Abcam. Anti-BRD3 (#A2277) antibody was purchased from Abclonal. Anti-Cyclin B1 (#sc-245) antibody was purchased from Santa Cruz. Anti-DAPK2 (#AW5377) antibody was purchased from Abgent (San Diego, CA). All antibodies were employed at suggested dilutions by the manufacturers. Anti-BRD3 (#A302-368A) antibody for Co-IP and ChIP assay was

purchased from Bethyl Laboratories (Germany). All the assays were performed according to the manufactory instructions.

**Histopathology and immunohistochemistry.** For routine histological analysis, lung lobes or tumor tissues were fixed in 4% buffered paraformaldehyde, dehydrated and embedded in paraffin. Sections of 3 μm thickness were subjected to haematoxylin and eosin staining and immunohistochemical staining. The staining lung lobes were scanned by the Leica ScanScope AT Turbo. The following primary antibodies were used: BCL6 (#ab172610, Abcam, 1:1500 dilution), Ki-67(#ab16667, Abcam, 1:5000 dilution), anti-phospho-S6$^{S235/S236}$ (#2211, CST, 1:100 dilution).

**Quantitative real-time PCR.** After drug-treatment or transfection for 48 h, cells were subjected to RNA extraction using the RNeasy kit (Qiagen). Subsequently, cDNA was synthesized using the PrimeScript RT reagent kit (TaKaRa). The cDNA was then subjected to PCR amplification using the SYBR Premix ExTaq kit (TaKaRa) on an Mx3005P thermal cycler (Stratagene) according to the manufacturer's instructions. The target mRNA expression was quantified using ΔΔCt method and normalized to GAPDH expression. PCR primers are listed in **Supplementary Table 8**.

**RNA sequencing.** RNA-seq experiment was performed as previously described(2). Briefly, total cellular RNA from DMSO- or OTX015-treated cells was individually extracted with TRIzol reagent (Invitrogen). Sequence reads were obtained using the SOLiD v4 sequencing platform. To identify differential expression, the RNA-seq reads were successfully mapped to the human genome without quality problems. Read counts were normalized, and fold changes were calculated for all possible comparisons. Transcripts with low abundance were filtered according to the previously described algorithm (3, 4). *P* value of 0.05 was used as a cutoff to select transcripts with good consistency. The selected transcripts were then overlapped with ChIP-seq candidate genes which harbor significant BCL6 binding signal within -2 kb ~ +0.2 kb around the transcript start sites. A

heat-map was shown to depict the fold changes of transcripts affected by OTX015 treatment.

**Two-dimensional clonogenic assay.** NSCLC cells were seeded onto 6 or 12-well plates (2,000~3,000 cells per well) and allowed to adhere overnight. Cells were then treated with indicated drugs for an additional 7 days. Medium with or without drugs was replaced every other day. Remaining cells were fixed with 4% paraformaldehyde and stained with 0.5% crystal violet and photographed. For analysis of cell viability of cultured colonies, staining was dissolved with 10% acetic acid, transferred to 96-well plates. The absorbance was read at a wavelength of 595 nm. Relative cell viability was calculated by setting untreated group as 100%.

**Soft-agar colony formation assay.** Two mL bottom layers containing 1.2% of low melting point agar (BD Biosciences, San Jose, CA) mixed with growth media was poured into wells of 6-well plates and allowed to set at room temperature. Cells were re-suspended in the second layer containing 0.5% of low melting point agar mixed with growth media and plated onto the previously prepared bottom layers (500 cells per well). Growth medium was added on top of the second layer, and cells were allowed to grow at 37 °C for an additional 3 days. Medium containing indicated drugs was then changed every other day. Representative colony images were recorded every 3 days. At the end of the experiment, colonies were counted and analyzed.

**Cell cycle analysis.** Cells were grown in 6 cm dishes and treated with indicated drugs or drug combinations for 48 h. Cells were then washed with PBS and fixed in 70% ethanol overnight. The cells were treated with 0.1% Triton X-100 and stained with propidiumiodide (Sigma). The cell cycle was analyzed by flow cytometry (FACS Calibur, BD).

**Safety testing in C57BL/6J mice.** To avoid potential toxicity in GEMM mice, we tested the safety of the co-treatment of OTX015 and FX1 in normal C57BL/6J mice. C57BL/6J mice were purchased from National Rodent Laboratory Animal Resources (Shanghai,

China). Mice were assigned in a randomized way to different treatment groups and treated with vehicle (2% DMSO + 5% Tween 80 + 30% PEG-400 in dd$H_2O$), OTX015 (50 mg/kg, orally, dissolved in 2% DMSO + 5% Tween 80 + 30% PEG-400 in dd$H_2O$), FX1 (12 mg/kg, intraperitoneally, suspended in 0.5% CMC-Na in sterile water) and OTX015 + FX1 for 3 weeks. On day 28, the mice were sacrificed, and relative mouse body weight was analyzed. The blood samples were collected by tail cutting and subjected to blood examination and plasma biochemistry testing (Shanghai ADICON Clinical Laboratories, Inc.).

## SUPPLEMENTAL METHODS REFERENCES


1. Chang Z, et al. Cooperativity of oncogenic K-ras and downregulated p16/INK4A in human pancreatic tumorigenesis. *PLoS One*. 2014;9(7):e101452.
2. Liu X, et al. Genome-wide Analysis Identifies Bcl6-Controlled Regulatory Networks during T Follicular Helper Cell Differentiation. *Cell Rep*. 2016;14(7):1735-1747.
3. Leach JP, et al. Hippo pathway deficiency reverses systolic heart failure after infarction. *Nature*. 2017;550(7675):260-264.
4. Tao G, et al. Pitx2 promotes heart repair by activating the antioxidant response after cardiac injury. *Nature*. 2016;534(7605):119-123.
5. Wang B, et al. The antiparasitic drug, potassium antimony tartrate, inhibits tumor angiogenesis and tumor growth in nonsmall-cell lung cancer. *J Pharmacol Exp Ther*. 2015;352(1):129-138.
6. Wang J, et al. Suppression of KRas-mutant cancer through the combined inhibition of KRAS with PLK1 and ROCK. *Nat Commun*. 2016;7:11363.